Chin. Phys. Lett. **39**, 026401 (2022) **Express Letter**

Evidence for a High-Pressure Isostructural Transition in Nitrogen

Chunmei Fan(范春梅)[1], Shan Liu(刘珊)[1], Jingyi Liu(刘静仪)[1], Binbin Wu(吴彬彬)[1], Qiqi Tang(唐琦琪)[1], Yu Tao(陶雨)[1], Meifang Pu(蒲梅芳)[1], Feng Zhang(张峰)[1], Jianfu Li(李建福)[2], Xiaoli Wang(王晓丽)[2*], Duanwei He(贺端威)[1], Chunyin Zhou(周春银)[3], and Li Lei(雷力)[1*]

[1]*Institute of Atomic and Molecular Physics, Sichuan University, Chengdu 610065, China*
[2]*School of Opto-Electronic Information Science and Technology, Yantai University, Yantai 264005, China*
[3]*Shanghai Synchrotron Radiation Facility, Shanghai Advanced Research Institute, Chinese Academy of Sciences, Shanghai 201204, China*

(Received 5 January 2022; accepted 19 January 2022; published online 23 January 2022)

We observed an isostructural phase transition in the solid nitrogen λ-N_2 at approximately 50 GPa accompanied by anomalies in lattice parameters, atomic volume and Raman vibron modes. The anomalies are ascribed to a slight reorientation of the nitrogen molecules, which does not seem to affect the monoclinic symmetry (space group $P2_1/c$). Our *ab initio* calculations further confirm the phenomena, and suggest an optimized structure for the λ-N_2 phase. In addition, a new high-pressure amorphous phase of η'-N_2 was also discovered by a detailed investigation of the pressure-temperature phase diagram of nitrogen with the aim of probing the phase stability of λ-N_2. Our result may provide helpful information about the crystallographic nature of dissociation transitions in diatomic molecular crystals (H_2, O_2, N_2, etc).

DOI: 10.1088/0256-307X/39/2/026401

High-pressure isostructural transitions (HPIT) are generally identified with symmetrical invariance in crystal structures, always signatured with the anomalies in cell volume, axial ratio and phonon behavior, possibly induced by the changes of the electronic states or by the slight displacements of atoms.[1−14] HPITs have been reported in metals such as Cd,[1] Zn[2,3] and Os,[4−6] metallic compounds like CaB_4[7] and MgB_2,[8] and molecular crystals such as H_2O,[9] NH_3,[10] ND_3,[11] H_2[12] and O_2.[13,14] As a simple type of homonuclear diatomic molecule, nitrogen exhibits similar high-pressure behavior with hydrogen and oxygen.[13−20] Owing to the strong N≡N covalent triple bonds, nitrogen becomes the most stable diatomic molecule and displays behavior of complex high-pressure phase transitions under high pressure.[21−42] Since the first report of nitrogen solids in the early last century, at least 20 solid nitrogen phases have been experimentally reported in a wide area of pressure-temperature (P–T) space.[22−38] Despite the important progress, additional work is needed to explain HPIT transitions. On the basis of previous works, the stability of lattice structure and electronic band dispersion components on compression are those key factors for occurrence of HPITs.[1−14]

As a high-pressure and low-temperature phase, monoclinic λ-N_2 ($P2_1/c$) may be the most stable solid molecular nitrogen.[41−44] The λ-N_2 can be formed by cold compression from liquid phase, once synthesized, it can stabilize between 5 to 105 GPa at 77 K, and from 30 to 150 GPa at 300 K, covering nine other ordinary phases in P–T space.[41−43] The formation of λ-N_2 was driven by a progressive reduction of the free rotation of the nitrogen molecules and therefore by the consequent lowering of the local symmetry. Low formation enthalpy and unique lattice structure make the distinct phase unique and very stable. However, the extraordinary phase stability of monoclinic λ-N_2 require an important attention and additional investigations are needed to study the structural arrangement of this phase. It is often controversial to identify newly discovered high-pressure isostructural transitions. *In situ* x-ray diffraction, high-pressure Raman scattering and *ab initio* calculations are the main three methods used to search for convincing evidence to support the HPIT theory.

In this work, we investigate the phase stability of λ-N_2 and revisit the phase diagram of nitrogen along six independent P–T experimental paths. The investigation of the structural vibrational information of solid nitrogen phases (λ-N_2, δ-N_2, δ_{loc}-N_2 and ε-N_2) is carried out by employing high-pressure angle dispersive x-ray diffraction (ADXRD) (three runs) and high-pressure Raman scattering (ten runs). *Ab initio* calculations are performed to analyze the structural properties and transition mechanism.

Frost *et al.*[41] first discovered the λ-N_2 using a theoretical structure predicted by Pickard and Needs[44] (space group $P2_1/c$; $a = 2.922$ Å, $b = 2.891$ Å,

*Corresponding author. Email: lei@scu.edu.cn; xlwang@ytu.edu.cn
© 2022 Chinese Physical Society and IOP Publishing Ltd

$c = 5.588$ Å and $\beta = 132.54°$ for lattice parameters; $x = 0.5678$, $y = 0.3764$ and $z = 0.4534$ for N fractional atomic coordinates at 40 GPa) for fitting the obtained experimental diffraction data. Nevertheless, we used the CALYPSO structure search algorithm and first principles calculations. Employing the software VASP, we demonstrated an optimized monoclinic structure (λ-N_2 with space group $P2_1/c$; $a = 2.9183$ Å, $b = 2.8934$ Å, $c = 5.5503$ Å and $\beta = 132.5177°$ for lattice parameters; $x = 0.0695$, $y = 0.3751$ and $z = 0.4540$ for N fractional atomic coordinates at 40 GPa) and structure is posted in Fig. 1(b). The complete methods in experiments and calculations are given in the Supplemental Material (SM). These two structures are very similar, the major difference seems to be the N fractional atomic coordinates. After the standardization of crystal data by using the Vesta software, the N fractional atomic coordinates are slightly different, and the major difference between these two structures is the β angle (see Table S1 in the SM). Our calculations show that the pressure dependences of unit cell volume (Fig. 2), enthalpy, band gap and N≡N bonding length (Figs. S4–S6 in the SM) of the two structures follow different trends. They are not exactly the same structure. As shown in Fig. 2, while Pickard's crystal parameters are expected to exhibit very good linear relationship with pressure, our crystal data demonstrates the existence of an obvious discontinuity at around 50 GPa.

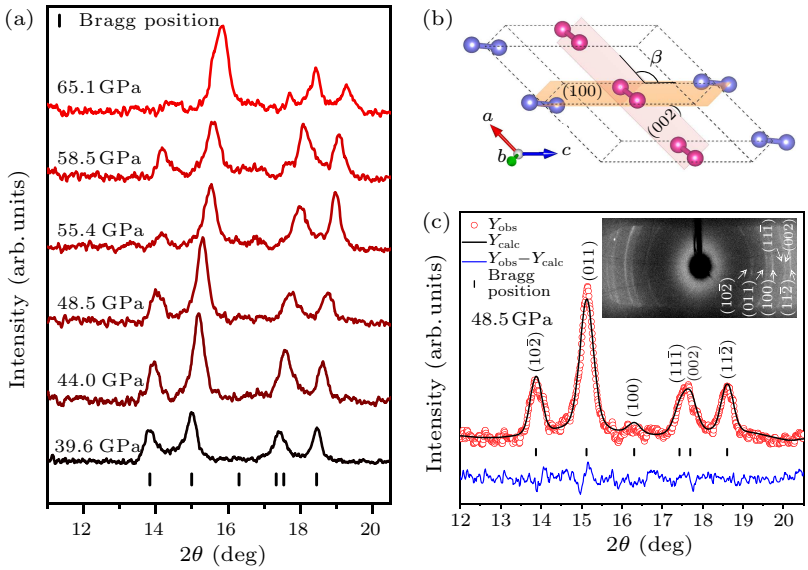

Fig. 1. X-ray diffraction data and structural information of λ-N_2. (a) X-ray diffraction patterns with the wavelength of 0.6199 Å on room-temperature compression. The arrows mark the diffraction peaks of gasket rhenium. (b) The re-optimized crystal structure of λ-N_2 with fractional atomic coordinates ($x = 0.0695$, $y = 0.3751$ and $z = 0.4540$). (c) Representative Rietveld-refined diffraction patterns with the corresponding unintegrated patterns (inset) for the λ-N_2 at 48.5 GPa.

As shown in Fig. 1(a), the five main Bragg diffraction peaks of λ-N_2 in experimental range from 10° to 22° can be followed from 35 to 65 GPa. All the observed peaks are found to shift towards higher angles without exhibiting peak broadening, as the pressure increases. This observation appears to indicate the presence of a decrease in the lattice-volume parameter without significant structural phase transitions. The diffraction peaks of gasket rhenium can be observed at higher pressures and their intensities increase with the applied pressure due to the shrinking of the sample cavity on compression. Due to the preferred orientation of the solid molecular phase under pressure, the diffraction peak along the (h00) direction cannot be clearly discerned.

We used both Pickard's crystal structure and our calculated structure for the λ-N_2 structural refinements.[44] High-quality refinements are shown in Fig. 1(c). Interestingly, the results display the presence of unusual features at approximately 50 GPa in the pressure dependence trend of atomic volume parameter. Noticeably, this effect is evident when considering the ratio of lattice parameters and the β angle (Figs. 2 and 3). We note that our calculated structure is more consistent with our experiment data than the initial model given by Pickard and Needs,[44] it is a more optimized structure for the λ-N_2.

The P–V relation on major molecular nitrogen phases is presented in Fig. 3(a). Our experimental data on λ-N_2, δ-N_2, δ_{loc}-N_2 and ε-N_2 are plotted together with data extracted from other literature reports (λ-N_2,[41,43] δ-N_2,[26] δ_{loc}-N_2,[29] ε-N_2,[26,30] ζ-N_2,[30] κ-N_2[32]) are also shown for comparison. Detailed analyses on δ-N_2, δ_{loc}-N_2 and ε-N_2 can be found

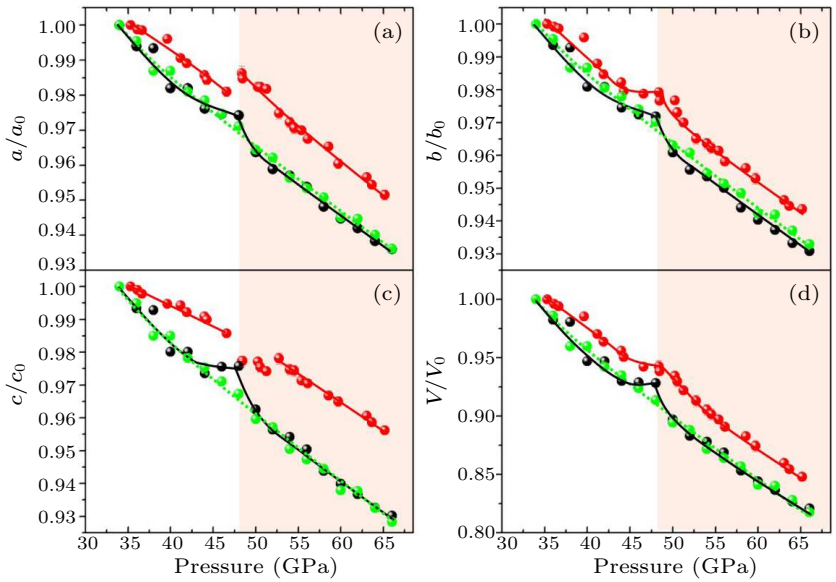

Fig. 2. The pressure dependence of a/a_0, b/b_0 and c/c_0 for the λ-N_2. The red circle represents the experimental data. The green and black circles represent calculation data with Pickar's and our structure, respectively. Solid and dashed lines are the guides for the eyes.

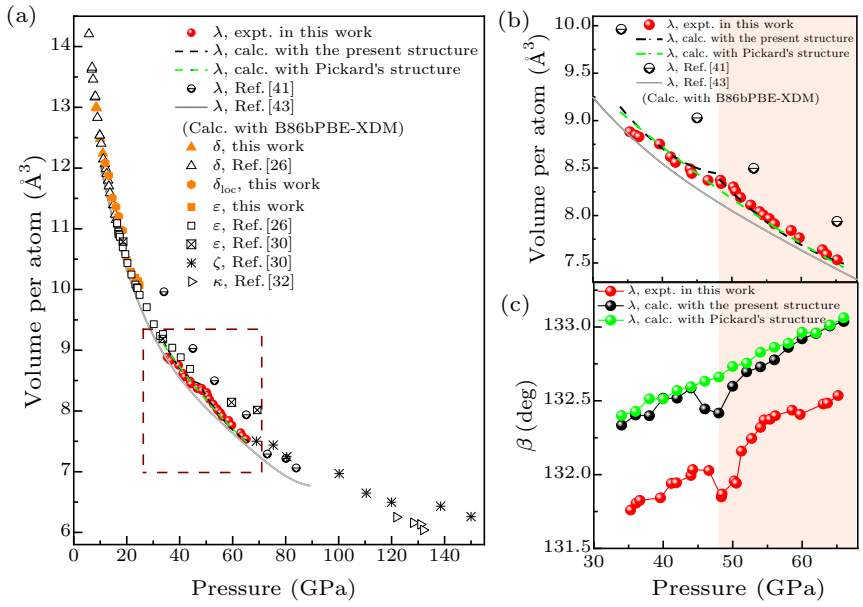

Fig. 3. Structural parameters of solid nitrogen under high pressure. (a) The P–V compression curves for the major molecular nitrogen phases. Solid shapes represent the present experimental data for λ-N_2, δ-N_2, δ_{loc}-N_2 and ε-N_2, respectively. The black dashed lines represent our calculation data for λ-N_2. Data from the literature are also shown for comparison, λ-N_2,[41,43] δ-N_2,[26] δ_{loc}-N_2,[29] ε-N_2,[26,30] ζ-N_2,[30] κ-N_2.[32] (b) The detailed area of the red frame is in Fig. 2(a). (c) The pressure dependence of β angle for the λ-N_2. The white and light red sections correspond to the change of anomalies region of λ-N_2. The data error bars are smaller than the data points shown in the figures.

in Figs. S1 and S2 in the SM. Figure 3(c) shows the compared β angle of λ-N_2 at various pressure as resulting from both experiment and theoretical calculations. The error bars of the experimental data are found to be smaller than the data points shown in the figures. The lattice parameter β angle is the degree between the (002) and (100) planes. Associated with the structural instability of molecular solid and orientation of the local molecular pairs, the β angle is a key parameter to evaluate the behavior of solid nitrogen at high pressure. Noticeably, without any change in the symmetry, the β angle does exhibit significantly discontinuous compressive behavior in both the experiment and theoretical calculation. The anomalies in the parameters of λ-N_2 seem to have no direct connection with the change of phonon dispersion and electronic states (Fig. S7). On the other hand, the volume of each nitrogen atom in λ-N_2 does not decrease smoothly with

the increase of the pressure parameters. A kink can be clearly observed at around 50 GPa [Fig. 3(b)]. In the regular room-temperature compression path, the phase transition from ε-N_2 to ζ-N_2 is expected to occur at about 56 GPa.[40] The slope change in the P–V curve at around 50 GPa underlines a discontinuity transition, possibly indicative of a transition in the λ-N_2. We note that only four valid XRD diffraction data for λ-N_2 were reported from 30 to 70 GPa in the literature.[41] The the discovery of the abnormal discontinuous trend evidenced by the structural parameters for λ-N_2 presented in this work is revealed in a large dataset, consisting into more than twenty-four available sets of acquired diffraction signals.

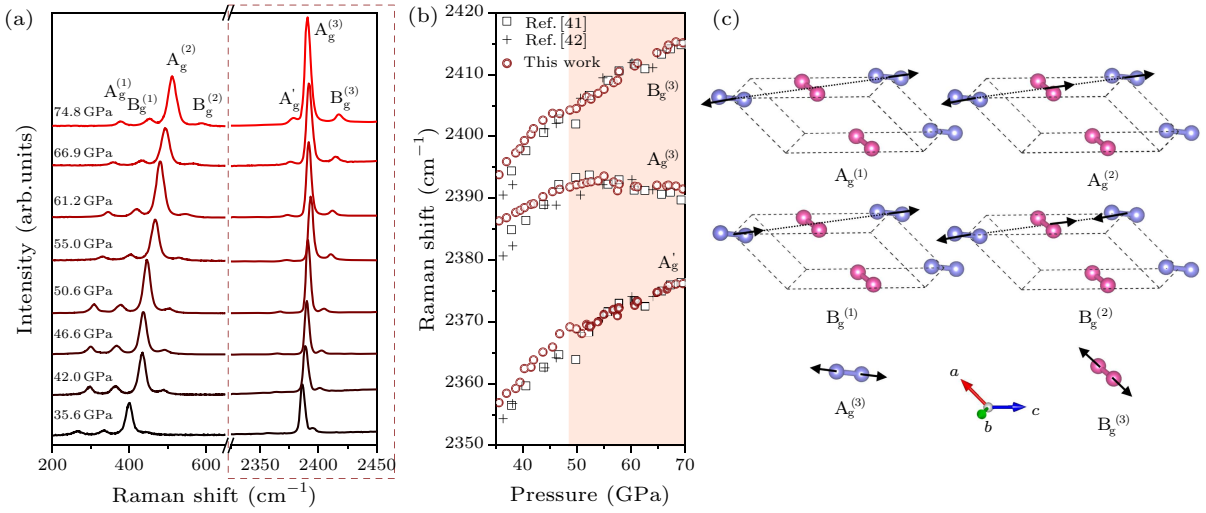

Fig. 4. (a) Representative Raman spectra of λ-N_2 on room-temperature compression. (b) High-frequency Raman peaks of the λ-N_2 as a function of the pressure at ambient temperature in experiments. The red circles are the present work. The hollow squares and vertical crosses represent previously reported experimental data.[41,42] (c) The atomic displacement diagram of λ-N_2 includes the $A_g^{(1)}$, $A_g^{(2)}$, $B_g^{(1)}$, $B_g^{(2)}$, $B_g^{(3)}$ and $B_g^{(3)}$ modes.

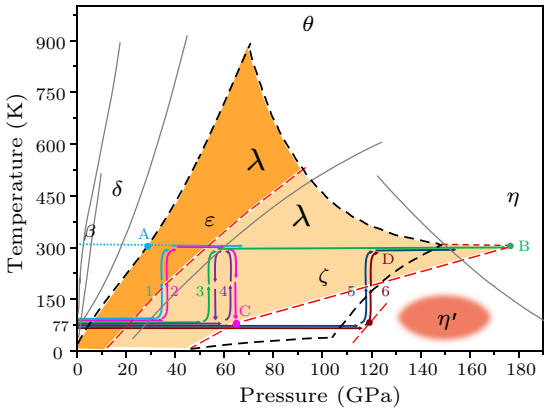

Fig. 5. Transformation and phase diagram of nitrogen. The deep orange section and lighter section are the forming region of λ-N_2. The red section is the region of η'-N_2. The six colorful lines represent different P–T paths to explore λ-N_2 formation and transition. The red dashed lines represent the revised transition boundaries of λ-N_2. The black dashed lines show the boundaries of λ-N_2 in Refs. [41,42]. The gray lines show the phase boundaries of nitrogen previously reported under compression at room temperature.

There are two types of diatomic molecular pairs with different orientations in the unit cell of λ-N_2 [Fig. 1(b)]. The blue molecular pairs in the edges of the unit cell are parallel to each other, whereas the red ones are in the center of the structure. The orientation stability of the polarized molecular pairs is prone to be distorted and the β angle is easier to be damaged at higher pressure (>30 GPa). The lattice modes do not exhibit such a strong broadening, this observation seems to imply that the reported phenomenon is related to the distortion of the molecule and not to nonhydrostatic conditions. By combining the careful structural refinements with our theoretical calculations, we propose that a monoclinic-to-monoclinic isostructural transition occurs in the λ-N_2. There are some potential structures for the λ-N_2,[43,44] and their enthalpies are quite close. It is possible that the abnormality of λ-N_2 at 50 GPa is due to the structural phase transition from Pickard's structure to the present structure. Considering our structure agrees better with the experimental results throughout the entire pressure region (Figs. 2 and 3), it is reasonable to conclude that our solution is the optimized structure for the λ-N_2.

The HPIT of λ-N_2 was also observed in high-pressure Raman scattering, and the subtle variation of high-frequency Raman shift with pressure is depicted in Fig. 4 (also see Fig. S3). As shown in Fig. 4(c), the low-frequency lattice phonon modes $A_g^{(1)}$, $B_g^{(1)}$, $A_g^{(2)}$ and $B_g^{(2)}$ are associated with the relative movement of nitrogen molecular pairs, and high-frequency vibron modes $A_g^{(3)}$ and $B_g^{(3)}$ are connected with the N≡N stretching vibrations for different nitrogen molecules,

and the A_g' is a disorder-activated Raman mode.[42] The three high-frequency vibrons show discontinuous changes in the vicinity of 50 GPa, but the kinks are found to emerge at different pressures, due to different vibration modes having distinct responses to the applied pressure.

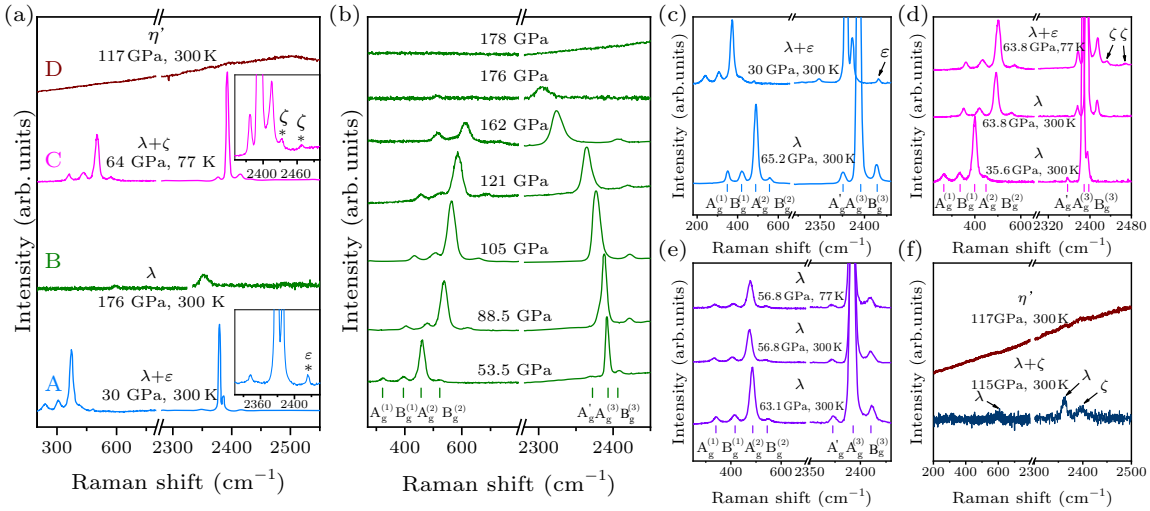

Fig. 6. (a) The Raman spectra correspond to the P–T points (A, B, C and D) in the P–T phase diagram. The selected Raman spectra along the path 3 (b), path 1 (c), path 2 (d), path 4 (e), paths 5 (upper) and 6 (lower) (f).

The transformation and phase diagram of nitrogen is shown in Fig. 6, six independent P–T paths via compression at 77 K up to at least 35, 36, 55, 61, 115 and 117 GPa are presented, which further refine the thermodynamic region of λ-N_2. The former P–T space of λ-N_2 in Refs. [41,42]. should be divided into two parts, a lower-pressure region for λ-N_2, a higher-pressure region for λ-N_2. In contrast with the previous work, our finding shows that λ-N_2 can be stabilized up to at least 176 GPa at room temperature, with a broadening and weakening Raman peaks [Fig. 6(b)]. When the external load pressure exceeds 178 GPa, all Raman peaks of λ-N_2 disappear and the sample becomes opaque. Once gained upon cooling to 77 K and at the pressure of 64 GPa, λ-N_2 and ζ-N_2 are found to coexist under the same P–T condition [see Fig. 6(d)]. Therefore, the low-temperature (77 K) boundary between λ-N_2 and ζ-N_2 should be down to 64 GPa, which is much lower than the previously reported pressure of 107 GPa in Ref. [42]. Noticeably, the λ-N_2 and ζ-N_2 were also found to coexist at pressure of 115 GPa and at $T \sim 300$ K [Fig. 6(f)]. This observation implies that the sample goes into a metastable region above 64 GPa and could continually keep up to 115 GPa at low temperature (77 K).

Together with the phase-transformations discussed above, it is also important to highlight presence of an extra component at 117 GPa and for $T \sim 77$ K. This new high-pressure nitrogen phase, referred to as η'-N_2, is found with significant inactivation in Raman bands [Fig. 6(f)]. It has not been verified whether η'-N_2 belongs to an amorphous phase like η-N_2. The reported amorphous η-N_2 can be obtained around 140 GPa at 300 K and has a large hysteresis, accompanied with the disappearance of the Raman signal and the emergence of a measurable resistance.[31,32] Interestingly, the η'-N_2 is easier to access at a lower pressure and room temperature through transformation of λ-N_2 probably owing to a minimization of the energetic barriers, with its unique structure.

In summary, the phase stability and structural information of the λ-N_2 have been investigated by high-pressure Raman scattering synchrotron x-ray diffraction, and *ab initio* calculations. A high-pressure monoclinic-to-monoclinic isostructural transition in the λ-N_2 has been observed at ~50 GPa supported by the discontinuous changes in lattice parameters and Raman vibrons, which is of the utmost importance for our physical understanding of such "simple" molecular systems and for benchmarking theoretical calculations.

Acknowledgments. We thank Professor Filippo Boi for helpful discussion. This work was supported by the Sichuan University Innovation Research Program of China (Grant No. 2020SCUNL107), the National Natural Science Foundation of China (Grant No. U2030107, 11774247, and 11974154), Chinese Academy of Sciences (Grant Nos. 2019-BEPC-PT-003237 and 2020-SSRF-PT-012109), and the Natural Science Foundation of Shandong Province (Grant Nos. 2019GGX103023 and Z2018S008).

References

[1] Pratesi G, Cicco A D, Minicucci M, and Itiè J P 2005 *J. Phys.: Condens. Matter* **17** 2625
[2] Li Z and Tse J S 2000 *Phys. Rev. Lett.* **85** 5130
[3] Kechin V V 2001 *Phys. Rev. B* **63** 045119

[4] Occelli F *et al.* 2004 *Phys. Rev. Lett.* **93** 095502
[5] Ma Y M *et al.* 2005 *Phys. Rev. B* **72** 174103
[6] Dubrovinsky L *et al.* 2015 *Nature* **525** 226
[7] Li G *et al.* 2014 *RSC Adv.* **4** 42523
[8] Sun L, Kikegawa T, Wu Q, Zhan Z, and Wang W 2001 *Chin. Phys. Lett.* **18** 1401
[9] Queyroux J A *et al.* 2020 *Phys. Rev. Lett.* **125** 195501
[10] Datchi F *et al.* 2006 *Phys. Rev. B* **73** 174111
[11] Ninet S *et al.* 2009 *Phys. Rev. B* **79** 100101(R)
[12] Ji C *et al.* 2019 *Nature* **573** 558
[13] Akahama Y, Kawamura H, Hausermann D, Hanfland M, and Shimomura O 1995 *Phys. Rev. Lett.* **74** 4690
[14] Freiman Y A, Jodl H J, and Crespo Y 2018 *Phys. Rep.* **743** 1
[15] Jiang S *et al.* 2018 *Nat. Commun.* **9** 2624
[16] Loubeyre P, Occelli F, and Dumas P 2020 *Nature* **577** 631
[17] Li Y W *et al.* 2018 *Nat. Commun.* **9** 722
[18] Shi X H, Liu B, Yao Z, and Liu B B 2020 *Chin. Phys. Lett.* **37** 047101
[19] Wu B B *et al.* 2021 *Matter Radiat. Extremes* **6** 038401
[20] Miao J Y, Lu Z S, Peng L, and Lu C 2021 *Chin. Phys. Lett.* **38** 066201
[21] Wang X L *et al.* 2012 *Phys. Rev. Lett.* **109** 175502
[22] Schuch A F and Mills R L 1970 *J. Chem. Phys.* **52** 6000
[23] Streib W E, Jordan T H, and Lipscomb W N 1962 *J. Chem. Phys.* **37** 2962
[24] Zinn A S, Schiferl D S, and Nicol M F 1987 *J. Chem. Phys.* **87** 1267
[25] Mills R L and Schuch A F 1969 *Phys. Rev. Lett.* **23** 1154
[26] Olijnyk H 1990 *J. Chem. Phys.* **93** 8968
[27] Scheerboom M I M and Schouten J A 1993 *Phys. Rev. Lett.* **71** 2252
[28] Hanfland M, Lorenzen M, Wassilew-Reul C, and Zontone F 1998 *Rev. High Press. Sci. Technol.* **7** 787
[29] Stinton G W, Loa I, Lundegaard L F, and McMahon M I 2009 *J. Chem. Phys.* **131** 104511
[30] Eremets M I *et al.* 2004 *J. Chem. Phys.* **121** 11296
[31] Gregoryanz E, Goncharov A F, Hemley R J, and Mao H K 2001 *Phys. Rev. B* **64** 052103
[32] Gregoryanz E *et al.* 2007 *J. Chem. Phys.* **126** 184505
[33] Gregoryanz E 2002 *Phys. Rev. B* **66** 224108
[34] Ma Y, Oganov A R, Li Z, Xie Y, and Kotakoski J 2009 *Phys. Rev. Lett.* **102** 065501
[35] Laniel D, Geneste G, Weck G, Mezouar M, and Loubeyre P 2019 *Phys. Rev. Lett.* **122** 066001
[36] Lei L, Tang Q Q, Zhang F, Liu S, Wu B B, and Zhou C Y 2020 *Chin. Phys. Lett.* **37** 068101
[37] Ji C *et al.* 2020 *Sci. Adv.* **6** eaba9206
[38] Laniel D *et al.* 2020 *Phys. Rev. Lett.* **124** 216001
[39] Eremets M I, Hemley R J, Mao H K, and Gregoryanz E 2001 *Nature* **411** 170
[40] Pu M F, Liu S, Lei L, Zhang F, Feng L H, Qi L, and Zhang L L 2019 *Solid State Commun.* **298** 113645
[41] Frost M, Howie R T, Dalladay-Simpson P, Goncharov A F, and Gregoryanz E 2016 *Phys. Rev. B* **93** 024113
[42] Liu S, Pu M, Tang Q Q, Zhang F, Wu B B, and Lei L 2020 *Solid State Commun.* **310** 113843
[43] Sontising W and Beran G J 2019 *Phys. Rev. Mater.* **3** 095002
[44] Pickard C J and Needs R J 2009 *Phys. Rev. Lett.* **102** 125702

Supplementary Material for "Evidence for a high-pressure isostructural transition in nitrogen"

Chunmei Fan(范春梅)[1], Shan Liu(刘珊)[1], Jingyi Liu(刘静仪)[1], Binbin Wu(吴彬彬)[1], Qiqi Tang(唐琦琪)[1], Yu Tao(陶雨)[1], Meifang Pu(蒲梅芳)[1], Feng Zhang(张峰)[1], Jianfu Li(李建福)[2], Xiaoli Wang(王晓丽)[2,*], Duanwei He(贺端威)[1], Chunyin Zhou(周春银)[3], and Li Lei(雷力)[1,*]

[1] *Institute of Atomic and Molecular Physics, Sichuan University, 610065 Chengdu, People's Republic of China*

[2]*School of Opto-Electronic Information Science and Technology, Yantai University, 264005 Yantai, People's Republic of China*

3, Shanghai Synchrotron Radiation Facility, Shanghai Advanced Research Institute, Chinese Academy of Sciences, Shanghai 201204, China

S-1. METHODS

High pressure was generated using a rheniums-gasket diamond anvil cell (DAC) with 100~300 μm culets. Solid nitrogen samples were successfully synthesized by compression of purity liquid and then warmed to ambient temperature for Raman and ADXRD experiments. High-pressure Raman scattering experiments were carried out using a custom-built confocal Raman spectrometry system in the back-scattering geometry excited by a solid-state laser at 532 nm. The sample pressure in Raman experiments were measured by the high-frequency edge of the diamond phonon [1, 2] and the ruby fluorescence method [3]. Considering that the ruby fluorescence scale method for the high pressure above 100 GPa cannot be read accurately, we only adopt the first-order diamond phonon [1, 2] as pressure calibration above 100 GPa. The

ADXRD experiments were collected at the 4W2 beam line of the Beijing Synchrotron Radiation Facility (BSRF, China) and the BL15U1 beam line of the Shanghai Synchrotron Radiation Facility (SSRF, China). The X-ray beam down to about $2.5\times2.5\ \mu m^2$ with 0.6199Å wavelength. The sample pressure in ADXRD experiments were measured using the high-frequency edge of the diamond phonon [1, 2], the ruby fluorescence method[3] and the equation of state (EOS) of rhenium [4]. The measured pressure error which used these methods is within 0.5 GPa (below 70 GPa). The two-dimensional diffraction patterns were analyzed with the programs Dioptas [5] and Fit2D [6], respectively. The structural refinements were performed by using software GSAS to get the lattice parameters [7].

The structures mentioned here were investigated by employing the swarm intelligence CALYPSO method [8, 9]. The total energy calculations and structure optimization were carried out using the plane wave basis, projected augmented wave (PAW) potentials, and generalized gradient approximation (GGA) with the Perdew-Burke Ernzerh (PBE) of exchange-correlation functional as implemented in the Vienna ab initio simulation package (VASP) [10-14]. The frozen-core all electron PAW potentials were used with $2S^2 2P^3$ treated as valence electrons for N. The Van der Waals density functional, namely optB86b-vdW, was adopted to treat dispersion forces. The cutoff energy (900 eV) for the expansion of the wave function into plane waves and Monkhorst-Pack [15] *k*-meshes (*k*-points density 0.02 $Å^{-1}$) are chosen to ensure that all the enthalpy calculations are well converged to better than 1 meV/atom. Using CALYPSO, we searched the

structures of nitrogen with simulation cell sizes of 1-40 formula units (f.u.) in the pressure range of 0-60 GPa. Phonon calculations were performed on the structures to determine their dynamic stability, by using a finite displacement approach as per the PHONOPY code [16, 17].

S-2. SUPPLEMENTARY DATA

	Original crystal data of Pickard's structure	Original crystal data in this work	Standardized crystal data of Pickard's structure	Standardized crystal data in this work
a/Å	2.9220	2.9183	2.9220	2.9183
b/Å	2.8910	2.8934	2.8910	2.8933
c/Å	5.5880	5.5503	4.6065	4.5919
β	132.5400	132.5177	116.6460	117.0130
V/Å^3	34.7806	34.5426	34.7806	34.5420
x	0.5678	0.0695	0.1610	0.1614
y	0.3764	0.3751	0.1236	0.1249
z	0.4534	0.4540	0.0466	0.0456

TABLE S1: The original and standardized crystal data of λ-N_2 in Ref [18] and the present work. The original data were standardized by using the Vesta software.

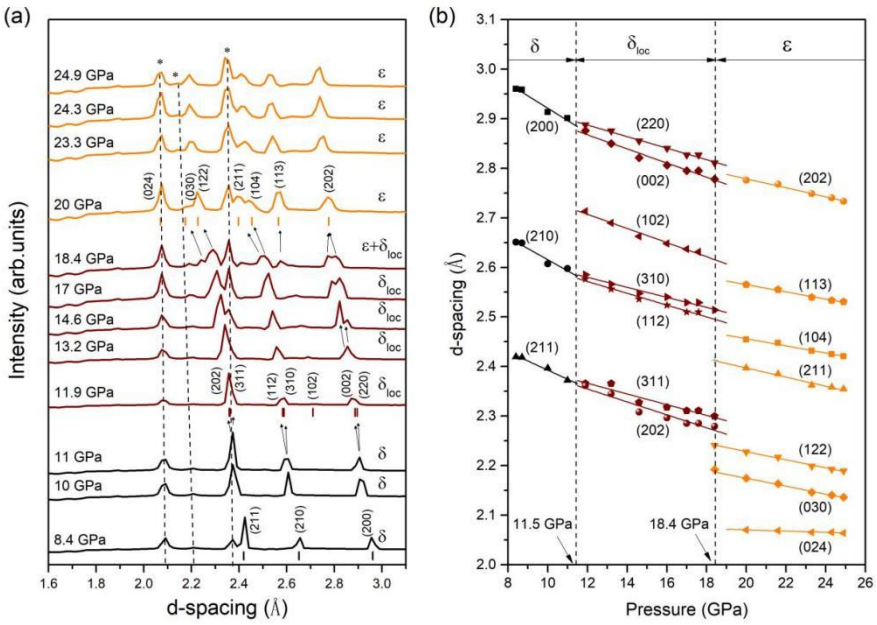

FIG.S1: (a) Integrated x-ray diffraction patterns of ordinary nitrogen phases collected at room temperature from 8.4 to 24.9 GPa at Beijing Synchrotron Radiation Facility (BSRF, China) with an X-ray wavelength of 0.6199 Å. The black dashed lines indicate the three diffraction lines of Re gasket, also identified at 24.9 GPa by black asterisks, which could be followed with pressure. Vertical bars indicated the *d* spacing positions. Nitrogen from 8.4 GPa to 11 GPa was identified as the δ-N_2 phase. The onset of the δ_{loc}-N_2 phase occurs at 11.5 GPa. The phase transition from δ_{loc} to ε occurs at 18.4 GPa. (b) The *d* spacings of the δ, δ_{loc}, and ε phases are presented as a function of pressure. The black dashed lines indicate the pressure boundary between these phases.

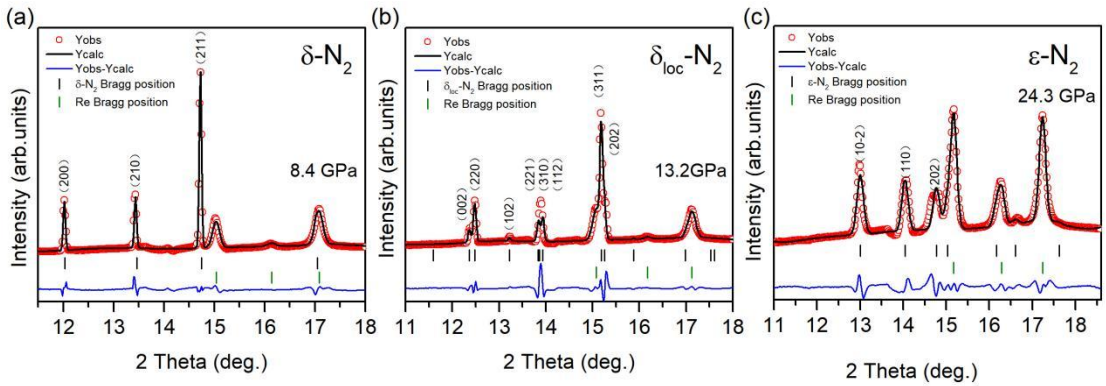

FIG. S2: Representative diffraction data and Rietveld-refined patterns of δ-N_2, δ_{loc}-N_2, and ε-N_2 at 8.4 GPa, 13.2 GPa, and 24.3 GPa, respectively. (a) The refinement results of δ-N_2 at 8.4 GPa: $a=b=c=5.9139$ Å, $R_{wp}=2.97\%$, $R_p=1.89\%$. (b) The refinement results of δ_{loc}-N_2 at 13.2 GPa: $a=b=8.1360$ Å, $c=5.7014$ Å, $R_{wp}=4.01\%$, $R_p=1.84\%$. (c) The refinement results of ε-N_2 at 24.3 GPa: $a=b=7.4349$ Å, $c=10.4038$ Å, $R_{wp}=5.70\%$, $R_p=6.90\%$.

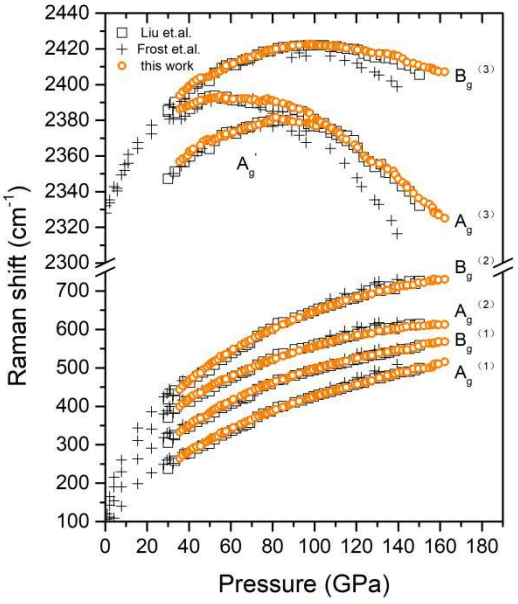

FIG. S3: The experimental Raman peaks of λ-N_2 at various pressures at room temperature in comparison with the data in the literature [19, 20]. The orange circles are the present data. The hollow squares and vertical crosses represent experimental data in the literature [19, 20].

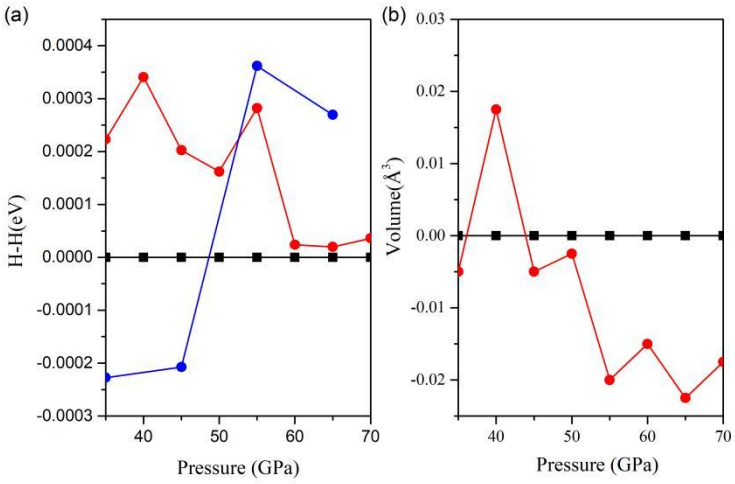

FIG. S4: (a) Enthalpy difference and (b) volume difference curves of the λ-N_2 around 50 GPa. The square and circles represent the data of Pickard's structure and the present structure, respectively. The red circles represent the calculated enthalpy without taking the zeor-point energy, and blue circles are the calculated data taking consideration of the zero-point energy.

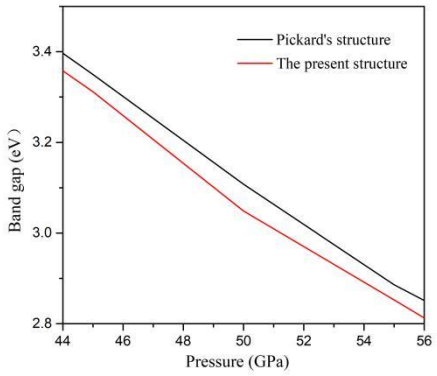

FIG. S5: The band gap of λ-N_2 with the two structures as a function of pressure.

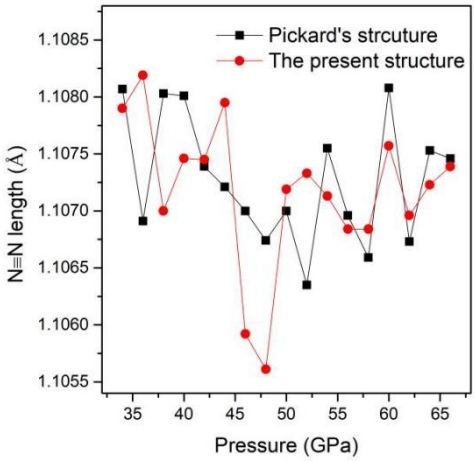

FIG. S6: The N≡N bonding length of λ-N_2 with the two different structures as a function of pressure.

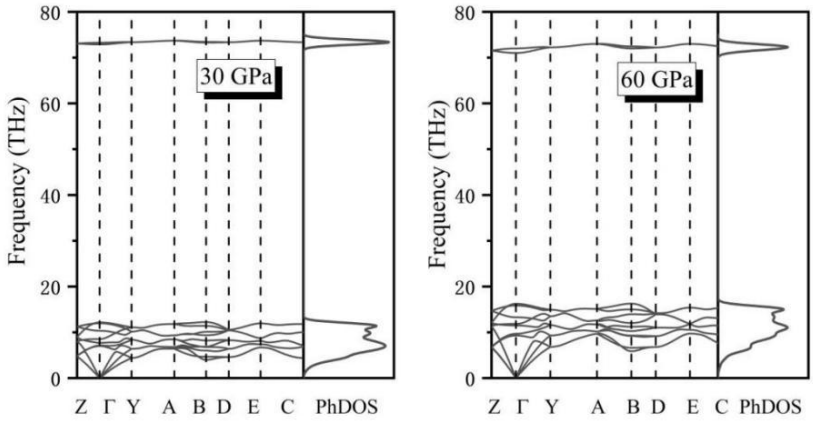

FIG. S7: Phonon dispersion and phonon DOS curves for λ-N_2 with our structure at 30 and 60 GPa, respectively.

1. Akahama Y and Kawamura H 2004 *J. Appl. Phys.* **96** 3748

2. Akahama Y and Kawamura H 2010 *J. Phys. Conf. Ser.* **215** 012195

3. Mao H K, Xu J and Bell P M 1986 *J. Geophys. Res.* **91** 4673

4. Zha C-S, Bassett W A and Shim S-H 2004 *Rev. Sci. Instrum.* **75** 2409

5. Prescher C and Prakapenka V B 2015 *High Pressure Res.* **35** 223

6. Hammersley A P, Svensson S O, Hanfland M, Fitch A N and Hausermann D 1996 *High Pressure Res.* **14** 235

7. Toby B H 2001 *J. Appl. Crystallogr.* **34** 210

8. Lv J, Wang Y, Zhu L and Ma Y 2011 *Phys. Rev. Lett.* **106** 015503

9. Wang Y, Lv J, Zhu L and Ma Y 2010 *Phys. Rev. B* **82** 094116

10. Kresse G and Furthmüller J 1996 *Phys. Rev. B* **54** 11169

11. Kresse G and Joubert D 1999 *Phys. Rev. B* **59** 1758

12. Dong W, Kresse G, Furthmüller J and Hafner 1996 J *Phys. Rev. B* **54** 2157

13. Blochl P E 1994 *Phys. Rev. B* **50** 17953

14. Perdew J P, Burke K and Ernzerhof M 1996 *Phys. Rev. Lett.* **77** 3865

15. Monkhorst H J and Pack J D 1976 *Phys. Rev. B* **13** 5188

16. Togo A, Oba F and Tanaka I 2008 *Phys. Rev. B* **78** 134106

17. The force constants matrix is determined by VASP. Convergence test gave the use of a $3 \times 3 \times 2$ supercell

18. Pickard C J and Needs R J 2009 *Phys. Rev. Lett.* **102** 125702

19. Frost M, Howie R T, Dalladay-Simpson P, Goncharov A F and Gregoryanz E 2016 *Phys. Rev. B* **93** 024113

20. Liu S, Pu M, Tang Q Q, Zhang F, Wu B B and Lei L 2020 *Solid State Commun*. **310** 113843